Rare Metal Materials and Engineering
Volume 52, Issue 10, October 2023
Available online at www.rmme.ac.cn

Science Press

Cite this article as: Xu Yangtao, Dai Jingmin, Pei Liang, et al. Comparison of Microstructure and Mechanical Properties of Electrodeposited Cobalt Plates[J]. Rare Metal Materials and Engineering, 2023, 52(10): 3387-3398.

ARTICLE

Comparison of Microstructure and Mechanical Properties of Electrodeposited Cobalt Plates

Xu Yangtao[1,2,3], Dai Jingmin[1,2], Pei Liang[1,2], Peng Yin[1,2], Du Haiyang[1,2]

[1] State Key Laboratory of Advanced Processing and Recycling of Nonferrous Metals, Lanzhou University of Technology, Lanzhou 730050, China; [2] School of Materials Science and Engineering, Lanzhou University of Technology, Lanzhou 730050, China; [3] Baiyin New Materials Research Institute, Lanzhou University of Technology, Baiyin 730900, China

Abstract: In order to study the differences in microstructure and mechanical properties of three kinds of electrodeposited cobalt plates, the preferred orientation, crystal structure, and microstructure of each plate were analyzed by X-ray diffractometer and scanning electron microscope. Furthermore, the mechanical properties of electrodeposited cobalt plates were tested, including their strength, hardness, and toughness. The results show that all of the plates are pure cobalt phases with a close-packed hexagonal structure (hcp) and random grain orientation. The deposition layer of the A-Co plate is uniform and dense with few holes, while those of the B-Co and C-Co plates grow apart and has a large number of holes. Meanwhile, the average grain size on the surface of the A-Co plate is the smallest, and the grain size distribution of the deposited layer is uniform, while that of the B-Co plate is the largest, and the grain size distribution of the deposited layer is not uniform. The starting sheets of the three electrodeposited cobalt plate cross-sections are all columnar crystal structures, and the growth patterns of the two sides of the starting sheets are different. From the analysis of mechanical properties, it is found that the tensile strength and hardness of the A-Co plate are higher than those of other two cobalt plates, but the toughness is lower. In conclusion, the quality of A-Co plates is significantly better than that of B-Co plates and C-Co plates.

Key words: electrodeposited cobalt; grain size; crystal structure; mechanical properties; preferred orientation

In recent years, the production of materials with novel structures and good properties by different techniques has become an important research goal[1]. As an important strategic reserve metal, cobalt is used in many fields because of its good corrosion resistance, wear resistance, thermal conductivity, magnetic properties, high temperature resistance, high hardness, and high strength[2–4], such as aerospace, electrical and electronic, mechanical manufacturing, chemical, and ceramic industrial fields[5]. It is therefore one of the most fascinating metallic materials for scientific and technological applications. Meanwhile, cobalt metal is also one of the important raw materials for manufacturing battery materials, cemented carbide, high-temperature alloys, magnetic materials, catalysts, and medical intermediates.

Electrochemical techniques have become an important platform for the preparation of coating materials with excellent mechanical properties[6]. Some researchers have found that a cobalt deposition layer can be coated on the surface of the material to improve properties[7]. In industrial production, the two methods for the production of pure metallic cobalt are hydrogen precipitation and electrolysis[8]. Since electrolysis is a low-cost, relatively simple method, suitable for low-temperature production, with high metal recovery rates, which also allows for large-scale production; and the average grain size of the material during electro-deposition can be simply adjusted by the applied current density, which will refine the average grain size to the nanometer scale[9]. And another advantage of producing pure metallic cobalt using electrolysis is the high purity of the prepared cobalt[10]. Therefore, electrolysis has become the dominant technology for producing various forms of cobalt metal. Nowadays, cobalt electro-deposition is receiving more

Received date: June 25, 2022
Foundation item: National Natural Science Foundation of China (52261011); Industrial Support Program for Higher Education Institutions in Gansu Province (2022CYZC-19); Gansu Province Key R&D Program Projects (21YF5GD186)
Corresponding author: Xu Yangtao, Ph. D., Professor, School of Materials Science and Engineering, Lanzhou University of Technology, Lanzhou 730050, P. R. China, Tel: 0086-931-2973939, E-mail: xuyt@lut.edu.cn

and more attention because of the special role of metallic cobalt in the field of materials.

The properties of the material depend on its microstructure, so it is particularly important to study the microstructure of electro-deposition cobalt to modulate its properties[11]. A fundamental challenge in the cobalt electro-deposition process is to control the structural morphology of the cobalt, while the structure and morphology depend on the conditions of preparation, such as electrolyte composition, electrolyte temperature, pH, current density, and additives[12]. Li[13] et al found that the deposited layers formed at lower temperatures and more positive cathodic potentials are uniform and dense, while deposited layers with non-uniform dendritic and cauliflower-like structures are formed, and the deposits are pure cobalt as shown by EDS and XRD analysis. Patnaik[14] et al investigated the effect of tetraethyl ammonium bromide (TEAB) on the structure and morphology of electrodeposited cobalt in aqueous sulfuric acid solutions and found that at low concentrations of TEAB (10 mg/L), the morphology of the cobalt deposited layers is uniformly dense, smooth, and bright, and when TEAB content exceeds 10 mg/L, the quality of the cobalt deposited layers becomes poor. Mahdavi et al discovered that adding 0.2 g/L sodium dodecyl sulfate to the electrolyte results in fewer defects in the deposited layer; adding saccharin makes the deposited layer smoother with finer grains, and adding 0.2 g/L sodium dodecyl sulfate and 0.5 g/L saccharin to the electrolyte at the same time makes the deposited layer dense, bright, and hard[15]. At present, there are relatively few studies on the microstructure and properties of cobalt deposited layers, so this study is intended to provide theoretical support for further improving the quality of electrodeposited cobalt plates by comparing and analyzing the microstructure and properties of three types of electrodeposited cobalt plates.

1 Experiment

The electrodeposited cobalt plates used in this study were all produced by the cobalt smelter production lines of A, B, and C companies in China, and the production cycle is about 5 d, the details of which are shown in Table 1.

A D8-ADVANCE type polycrystalline X-ray diffractometer was used to analyze the crystal structure and preferred orientation of three kinds of electrodeposited cobalt plates. The surface microstructure morphology and fracture morphology of Co plates were observed by a Quanta 450 FEG field emission scanning electron microscope, and the specimen size was 10 mm×10 mm. Before the experiment, the prepared corrosion solution (5 g $FeCl_3$+50 mL HCl+100 mL deionized water) was evenly wiped to the detection surface of the specimen and wiped for about 30 s. The crystallographic information, such as grain size and orientation difference of the surface and cross-section of the three electrodeposited cobalt plates, was analyzed using a scanning electron microscope equipped with an Oxford-SYMMERY type EBSD analyzer.

Table 1 Electrodeposited cobalt plates of three different companies

Plate	Main preparation process	Thickness/mm	Specification
A-Co	Electro-deposition	4–7	Co9995
B-Co	Electro-deposition	4–7	Co9995
C-Co	Electro-deposition	3–5	Co9995

In order to make the experimental results more scientific and accurate, the tensile specimens, impact specimens, and micro-Vickers hardness test specimens were taken from different positions (upper, middle, and lower) and different directions (horizontal and gravity directions) along the diagonal position of the electrodeposited cobalt plates. Tensile tests were performed on a microcomputer-controlled electronic universal testing machine at a stretching speed of 5 mm/min with a standard sample according to "GB/T 228.1-2020". The impact specimen is a Charpy V-notch impact specimen of 55 mm×10 mm×H (H is the thickness of the cobalt plate specimen; its value is taken as 5 or 2.5 mm) processed in accordance with the national standard "GB/T 229-2020". Due to the difference in the thickness of the cobalt plates, the A-Co and B-Co plates were processed into specimens with a thickness of 5 mm, and the C-Co plates were processed into specimens with a thickness of 2.5 mm, and then tested on a ClEM-30D-CPC type electronic measurement impact tester. Micro Vickers hardness was tested on a model 1102D37 Wilson automatic micro hardness tester.

2 Results and Discussion

2.1 Phase and preferred orientation

Fig. 1 shows the XRD patterns of the surfaces and cross sections of three electrodeposited cobalt plates. By comparing the experimental results with the PDF (05-0727) cards of the standard diffraction peaks, it is found that the space groups are all P63/mmc (194) and the unit cell fundamental vector parameters are a=b=0.250 31 nm, c=0.406 05 nm, a=b≠c, α=β=90°, γ=120°. This shows that all three electrodeposited cobalt plates are pure cobalt phase (α-Co) with a close-packed hexagonal structure (hcp). In the patterns, diffraction angles of 41.51°, 44.46°, 47.37°, 75.76°, 84.18°, and 95.47° correspond to the crystal planes of $(10\bar{1}0)$, (0002), $(10\bar{1}1)$, $(11\bar{2}0)$, $(10\bar{1}3)$, and $(11\bar{2}2)$, respectively; they are highly coincident with the angles at which the pure cobalt phase appears.

In order to obtain the preferred orientation of different crystal faces, the calculation was performed using the parameter TC (texture coefficient) with the following equation[16]:

$$TC = \frac{\left[I_{hkl}/I^0_{hkl}\right]}{\sum\left(I_{hkl}/I^0_{hkl}\right)} \times 100\% \quad (1)$$

where I_{hkl} is the measured diffraction peak intensity, and I^0_{hkl} is the intensity of the standard diffraction peak. The texture coefficients of each crystal face of three electrodeposited cobalt plates calculated by Eq.(1) are shown in Table 2. If the TC value of one crystal face is higher than the average value, it means that the crystal face is in the preferred orientation, and if the TC value is larger, it means that the degree of

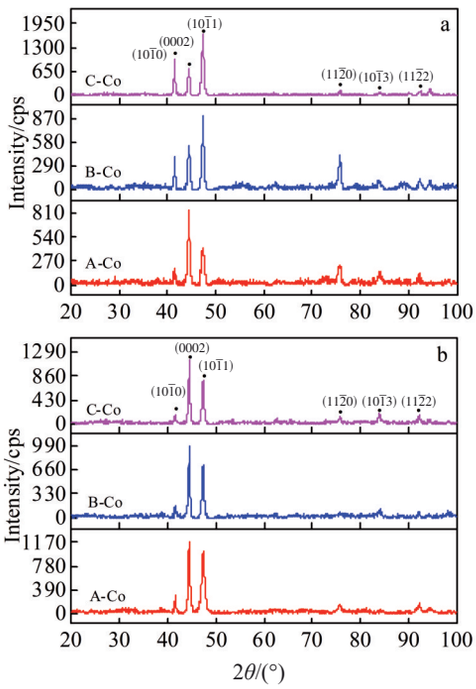

Fig.1 Surface (a) and cross-sectional (b) XRD patterns of three electrode-posited cobalt plates

Table 2 Texture coefficient (TC) of three electrodeposited cobalt plates (%)

Plate	Crystal face	(10$\bar{1}$0)	(0002)	(10$\bar{1}$1)	(11$\bar{2}$0)
A-Co	Surface	26.3	49.2	14.9	9.7
	Cross-section	32.8	42.7	21.0	3.5
B-Co	Surface	46.6	20.6	20.7	12.0
	Cross-section	23.6	51.6	22.6	2.3
C-Co	Surface	62.0	15.4	20.7	1.8
	Cross-section	20.2	54.5	22.2	3.1

preferred orientation in the crystal face is higher. As shown in Fig. 1, there are six crystal planes; for experimental accuracy, three strong peaks are taken for analysis, so the average value of TC is 25%.

According to the texture theory of electro-deposition[17], it is known that the initial stage of electro-deposition is dominated by epitaxial growth, followed by the common control of epitaxial growth and electro-deposition conditions. The thickness of the deposited layer gradually increases as the electro-deposition process proceeds, and the growth of the cobalt deposited layer is completely controlled by the electro-deposition conditions[18]. However, since the arrangement of atoms on different crystalline surfaces is different, the electrochemical activity will also differ, resulting in different growth rates for crystalline surfaces. The data in Table 2 show that both the surface and cross section of the A-Co plates show an obvious double preferred orientation on both the (10$\bar{1}$0) surface and the (0002) surface. The surfaces of the B-Co and C-Co plates exhibit an obvious preferred orientation on the (10$\bar{1}$0) face, while the cross section exhibits an obvious preferred orientation on the (0002) face. Because the current cobalt electro-deposition process is at a confidential stage, it is unknown which of the process parameters, such as temperature, pressure, concentration, and environment, influences the preferred orientation of the cobalt deposited layer, and further studies are needed[19].

2.2 Grain size calculation

Scherrer's formula was used to calculate the grain sizes of three kinds of electrodeposited cobalt plates. The formula is as follows[20]:

$$D_{hkl} = \frac{K\lambda}{\beta\cos\theta} \quad (2)$$

where D_{hkl} is the grain diameter (nm) along the direction perpendicular to the crystal face (hkl); β is the half-height width of the diffraction peak; θ is the diffraction angle; λ is the X-ray wavelength, and the value is 0.154 06 nm; K is a constant, and its value is taken as 0.89.

The calculated grain sizes of the three electrodeposited cobalt plates are shown in Table 3. It can be seen from the data that the average grain size of A-Co plates is about 18.51 nm, and that of B-Co and C-Co plates plates is about 22.02 and 21.40 nm. From the perspective of their average grain size, the grain size of A-Co plates is smaller than that of the

Table 3 Grain size (D_{hkl}) of the three electrodeposited cobalt plates (nm)

Plate	Crystal face	(10$\bar{1}$0)	(0002)	(10$\bar{1}$1)	(11$\bar{2}$0)	Average
A-Co	Surface	21.07	20.22	16.86	13.33	17.87
	Cross-section	25.63	20.03	13.93	17.00	19.15
B-Co	Surface	27.47	19.39	20.49	18.17	21.38
	Cross-section	29.60	23.20	17.70	20.11	22.65
C-Co	Surface	21.89	19.57	17.96	24.25	20.92
	Cross-section	23.55	23.92	17.06	20.08	21.15

other two Co plates.

2.3 Microstructure

2.3.1 Surface microstructure

Fig. 2 shows the SEM surface morphologies of three electrodeposited cobalt plates. It is seen that the deposited layer of A-Co plates is uniform, dense, and fine, with only minor holes present (as shown in Fig.2a and 2d). Both of the B-Co and C-Co plates are composed of ridge steps, most of which are parallel to the surface and pyramid-shaped, with a relatively scattered shape distribution, and local areas appear to have colony-like morphology aggregated by tiny pyramidal structures. It is suggested that in the process of electrodeposition, the colony-like morphology is then accumulated and grown by the continuous aggregation of reduced cobalt atoms, which fully accords with the island growth theory[21]. However, both types of electrodeposited cobalt plates have a large number of holes, which may be due to the fact that the pyramid particles are joined and merged with each other into a new particle during the growth process, leading to the formation of hole defects between them[9]. According to the microscopic morphology of three electrodeposited cobalt plates and combined with XRD analysis, it is found that the preferred orientation of the grain growth of their deposited layers will have a certain influence on their microscopic morphology.

Fig.3 shows the grain morphologies and phase diagrams of the surface for three electrodeposited cobalt plates. From Fig.3a–3c, it can be seen that the grain morphologies of the three electrodeposited cobalt surfaces are all equiaxed crystal, but the A-Co and C-Co plates have finer grains than the B-Co plates, and the grain size of these two companies is relatively more uniform. According to the statistical results in Fig.4, the average grain size of A-Co plates is 0.381 71 μm with a standard deviation of 0.460 28 μm; that of B-Co plates is 0.498 16 μm with a standard deviation of 0.665 28 μm; and that of C-Co plates is 0.409 16 μm with a standard deviation of 0.5078 μm. It can be seen that the average grain size and standard deviation value of A-Co plate are the smallest, and the standard deviation reflects the dispersion degree of a data set, so the small standard deviation indicates that the grain size of the A-Co plate surface is more uniform. The average grain size and standard deviation of the B-Co plate are larger, indicating that the grain size of the surface of the B-Co plate is relatively non-uniform, while the average grain size and standard deviation of the C-Co plate are between those of the A-Co plate and the B-Co plate. However, there is a difference between the average grain size calculated by EBSD statistics and Scherrer's formula from the data obtained by X-ray diffraction. There are two possible reasons for this difference. On the one hand, because the same orientation grains are marked in the same color during the EBSD test and there may be sub-grain boundaries between grains with the same orientation, these sub-grain boundaries are not identified during the test due to the influence of the calibration point step, which results in a large average grain size. On the other hand, the X-ray diffractometer itself will broaden the width of the diffraction peaks of nanomaterials in the process of testing and the broadening will cause the half-height width of the diffraction peaks to increase, which will result in smaller results after the calculation by bringing Scherrer's formula, and the effect of this broadening cannot be completely eliminated in the experimental process[22–23]. At the same time, the range of Scherrer's formula is 1–100 nm. If it is greater than this range, the calculation of grain size by Scherrer's formula has lost its meaning. Therefore, in this study, the grain size of three electrodeposited cobalt plates is calculated

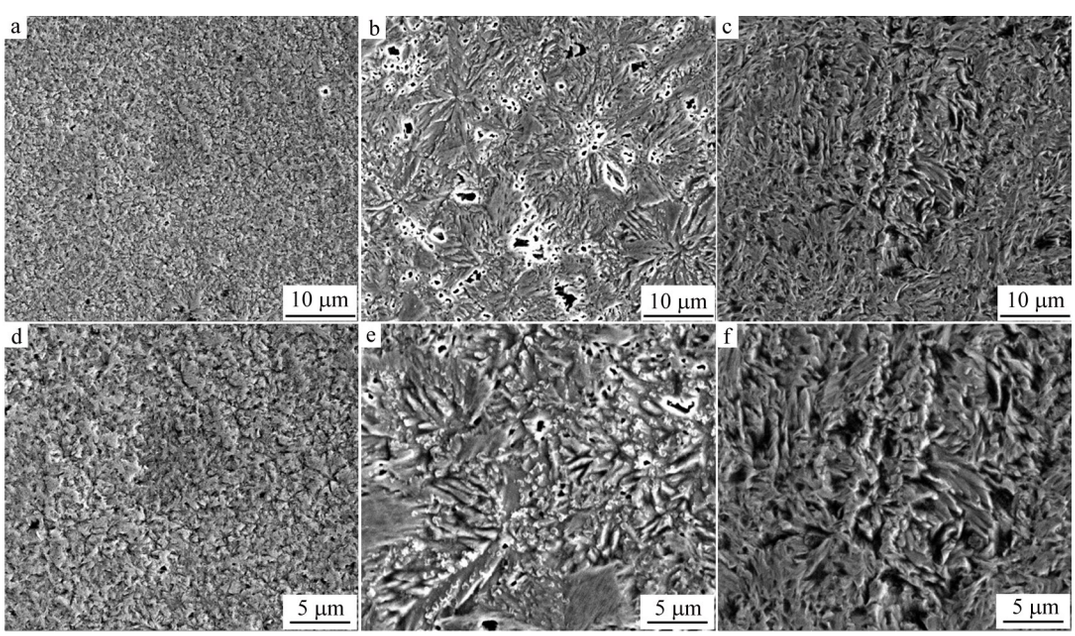

Fig.2 SEM surface morphologies of three electrodeposited cobalt plates: (a, d) A-Co; (b, e) B-Co; (c, f) C-Co

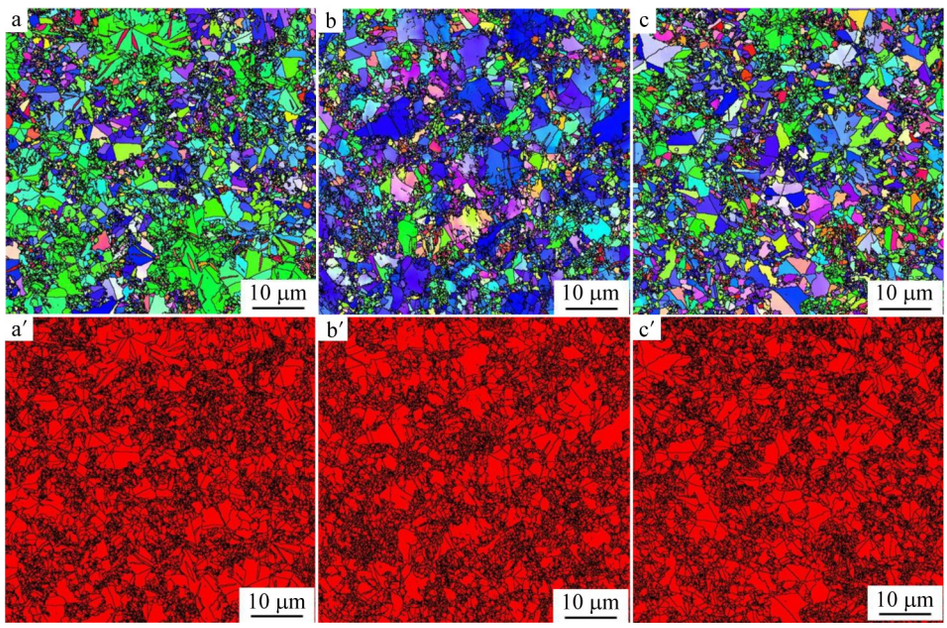

Fig.3 EBSD surface morphologies and phase diagrams of three electrodeposited cobalt plates: (a, a′) A-Co; (b, b′) B-Co; (c, c′) C-Co

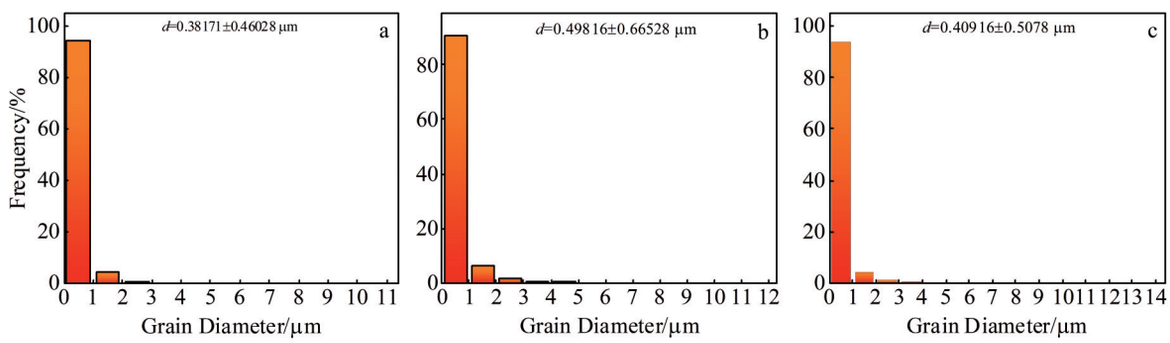

Fig.4 EBSD surface grain size statistics of three electrodeposited cobalt plates: (a) A-Co, (b) B-Co, and (c) C-Co

with the aid of Scheele's formula in order to see the trend of grain size, mainly based on the results of EBSD. Also from the phase diagrams of three electrodeposited cobalt plates (Fig.3a′–3c′), it can be seen that they are all composed of α-Co phases with close-packed hexagonal structures (hcp), which is consistent with the previous XRD experimental results.

The distribution of surface grain boundary characteristics and the distribution of grain boundary orientation differences for three electrodeposited cobalt plates are shown in Fig. 5. The grain boundaries with adjacent grain orientation difference less than 15° belong to small angle grain boundaries, while sub-grain boundaries also belong to small angle grain boundaries, and generally the adjacent orientation difference is less than 2°, whereas the grain boundaries with adjacent grain orientation difference greater than 15° are called large-angle grain boundaries. Small-angle grain boundaries are shown by red lines, and large-angle grain boundaries are shown by black lines. From the orientation difference distribution chart, we can see that the orientation difference of A-Co plates is mainly concentrated in the small angle range (less than 5°), about 65°, and about 87°, among which the percentage of sub-grain boundaries (less than 2°) is 29%, the percentage of small angle grain boundaries with an orientation difference of 2° to 15° is 13%, and the percentage of large-angle grain boundaries with an orientation difference greater than 15° is 58%. The orientation difference of B-Co plates is mainly concentrated in the small angle range (less than 6°), while the percentage of sub-grain boundaries (less than 2°) is 42%; the percentage of small-angle grain boundaries with an orientation difference of 2° to 15° is 21%, and the percentage of large-angle grain boundaries with an orientation difference greater than 15° is 37%. The orientation difference of C-Co plates is similar to that of A-Co plates, which is also mainly concentrated in the small angle range (less than 5°), about 65° and 87°, where the sub-grain boundary (less than 2°) accounts for 32%, the small-angle grain boundary with an orientation difference from 2° to 15° accounts for 13%, and the large-angle grain boundary with an orientation difference greater than 15° accounts for 55%. The comparison shows that the large-angle grain boundaries of A-Co and C-Co

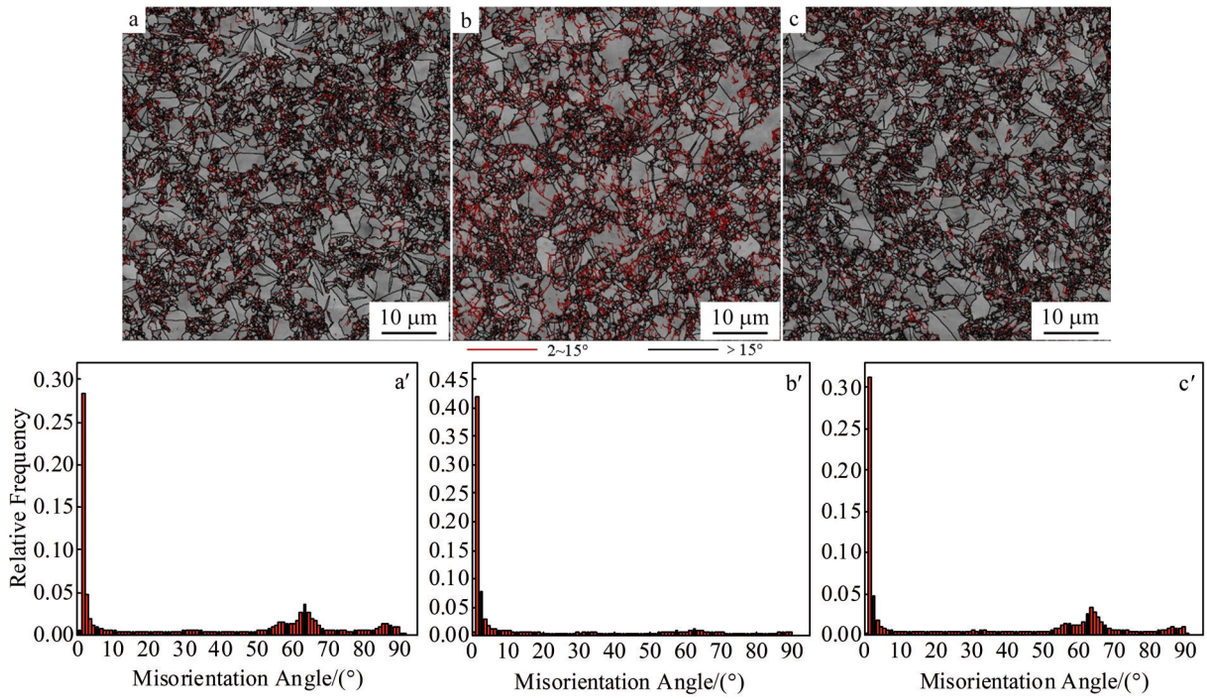

Fig.5 Surface grain boundary characteristic distribution and grain boundary orientation difference distribution of three electro-deposited cobalt plates: (a, a′) A-Co; (b, b′) B-Co; (c, c′) C-Co

plates are significantly higher than those of B-Co plates, and the higher the proportion of large-angle grain boundaries, the smaller the average grain size of the deposited layer, and the higher the strength and the hardness. This is mainly due to the higher interfacial energy of large-angle grain boundaries compared to small-angle grain boundaries and the irregular arrangement of atoms at grain boundaries, whereas the existence of grain boundaries will play a hindering role in the movement of dislocations, resulting in increased plastic deformation resistance, which is macroscopically manifested in higher strength and hardness of the material[24].

2.3.2 Cross-sectional microstructure

Fig. 6 shows the cross-sectional morphology of the starting sheet. It can be seen that the middle is the region of the starting sheet, and the thickness is about 0.6 mm, while both sides of the starting sheet are the region of the deposition layer. The contact between two sides of the deposited layer area and the starting sheet is different because the starting sheet is produced with a titanium plate as the mother plate, and after the deposition is completed, the starting sheet needs to be directly peeled off from the mother plate, then leveled and cut to the edge as the cathode for electrolytic deposition, while the surface on this side peeling off from the titanium plate is relatively flat and smooth (the left dividing line in Fig. 6), and the other side of the rough surface is a free-deposited surface obtained by electrolytic deposition[25]. Moreover, it can be seen from that the left-side demarcation line is more obvious, while the right-side demarcation line is not very obvious, indicating that the free deposition surface of cobalt on the right side of the starting piece continues the growth mode of the matrix so that its demarcation line is not very obvious.

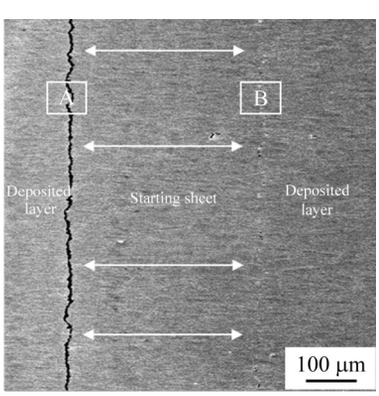

Fig.6 Cross-sectional SEM morphology of starting sheets of electrodeposited cobalt plates

Fig.7 shows the EBSD cross sections morphologies of three electrodeposited cobalt plate. Fig.7a, 7c, and 7e correspond to region A in Fig. 6, while Fig. 7b, 7d, and 7f correspond to region B in Fig.6. It can be seen that all the starting sheets of the three electrodeposited cobalt plates are composed of columnar crystals, and the starting sheets of the A-Co and C-Co plates have a more uniform morphology. The starting sheets on the left side of the B-Co plate have relatively small grains, while the grains of the right side are obviously coarse. Meanwhile, a clear demarcation line can be seen in the region of the deposited layer on the left side of the three electrodeposited cobalt plates near the starting sheet, which is

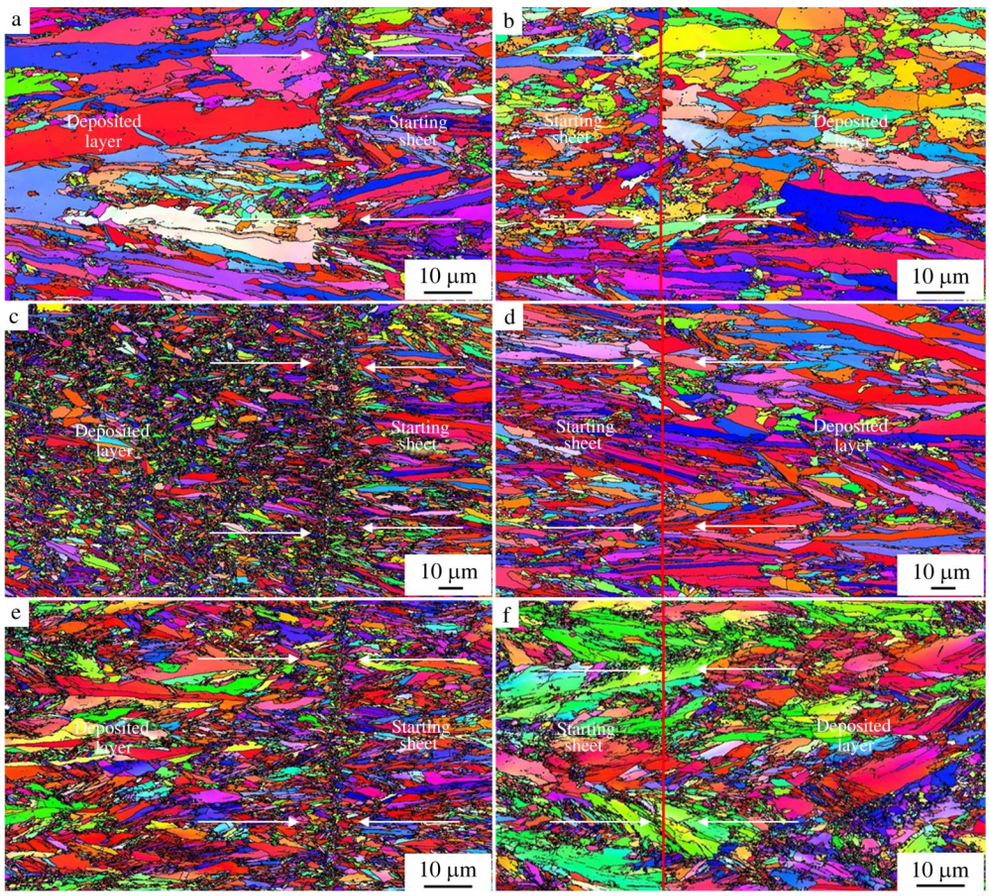

Fig.7 EBSD cross-sectional morphologies of three electrodeposited cobalt plates: (a, b) A-Co; (c, d) B-Co; (e, f) C-Co

consistent with the results observed by SEM and is composed of many fine equiaxed crystals at the binding site between the starting sheet and the deposited layer. With the extension of the deposition time, the deposition layer on the left side of the A-Co plate gradually changes from many fine equiaxial crystals to coarse columnar crystals growing outward, that of the B-Co plate grows in a way that many fine equiaxial crystals are mixed with a few columnar crystals, while that of the C-Co plate gradually changes from fine equiaxial crystals to many coarse columnar crystals and a few equiaxial crystals growing outward. It can be seen that the deposited layer of the three electrodeposited cobalt plates near the left starting sheet does not continue the growth pattern of the matrix but re-nucleates on the surface of the matrix. This is because at the binding site on the left side, the grains are relatively small and the atomic arrangement is disturbed, which leads to re-formation nucleation on the surface of the matrix and the appearance of a clear demarcation line.

The boundary line between the deposition layer on the rightside of the three electro-deposited cobalt plates and the starting sheet is not visible, and the two parts are almost integrated, indicating that the right deposition layer continues the growth pattern of the starting sheet, all of which grow outward in the way of columnar crystals on the starting sheet, and the morphology of the right deposition layer is uniform. However, it can be seen that the columnar crystals on the right deposition layer of A-Co and C-Co plates are relatively coarse, while the right deposition layer of B-Co plate is composed of elongated columnar crystals, which may be caused by different additives added during the production process.

2.4 Tensile test at room temperature

2.4.1 Tensile strength of three electrodeposited cobalt plates

The stress-strain curves of the three electrodeposited cobalt plates in different directions and different positions are shown in Fig.8. As can be seen, they have no obvious upper or lower yield points; for metallic materials without obvious yield points, the stress value at which a residual strain of 0.2% is generated is specified as their yield limit and called as the conditional yield limit or yield strength[26]. An analysis of the data obtained from Table 4 shows that there are certain differences in the tensile strengths of the three electro-deposited cobalt plates in different directions and different positions. The tensile strength of A-Co plates is 1014 MPa in the horizontal direction and 1071 MPa in the gravity direction. The tensile strength of B-Co plates is 783 MPa in the horizontal direction and 805 MPa in the gravity direction, but it is found from the tensile strength of B-Co plates in Table 4 that the tensile strengths in different directions and locations are relatively uniform. Meanwhile, the tensile strength of C-Co plates is 810 MPa in the horizontal direction and 858 MPa

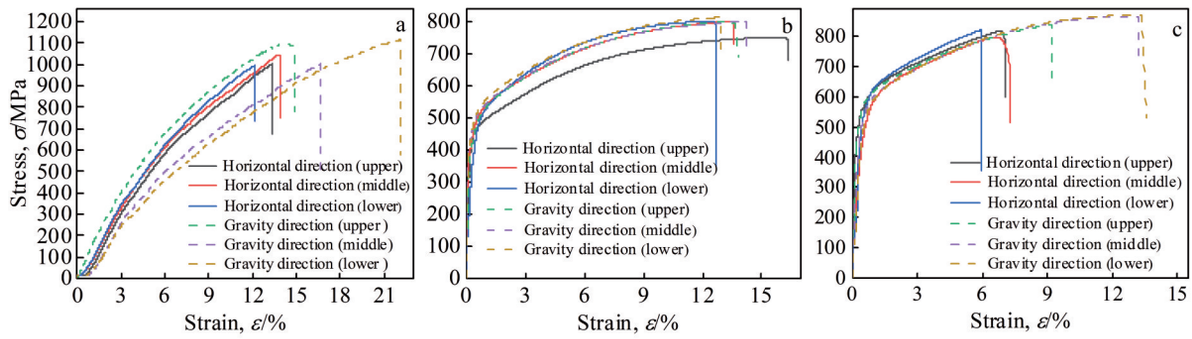

Fig.8 Stress-strain curves of three electrodeposited cobalt plates in different directions and different positions: (a) A-Co, (b) B-Co, and (c) C-Co

Table 4 Room temperature tensile porperties of three electrodeposited cobalt plates

Plate			Cross-sectional area/mm^2	Yield strength, $R_{p0.2}$/MPa	Tensile strength, R_m/MPa
A-Co	Upper	Horizontal direction	39.41	670	1002
		Gravity direction	40.00	892	1095
	Middle	Horizontal direction	40.04	706	1043
		Gravity direction	38.43	616	1003
	Lower	Horizontal direction	39.50	658	998
		Gravity direction	39.66	810	1115
B-Co	Upper	Horizontal direction	38.59	500	750
		Gravity direction	38.46	455	800
	Middle	Horizontal direction	38.68	455	800
		Gravity direction	37.99	445	800
	Lower	Horizontal direction	38.31	490	800
		Gravity direction	38.40	455	815
C-Co	Upper	Horizontal direction	39.50	555	815
		Gravity direction	38.37	540	865
	Middle	Horizontal direction	38.02	540	795
		Gravity direction	38.65	575	840
	Lower	Horizontal direction	37.40	620	820
		Gravity direction	38.50	560	870

in the gravity direction. It can be seen that the tensile strength in the direction of gravity is greater than in the horizontal direction for all three types of electrodeposited cobalt plates, mainly because in the process of producing electrodeposited cobalt plates, it is placed vertically. In this process, due to the effect of gravity, the cobalt atoms deposit a denser texture in the direction of gravity. Therefore, more energy is needed in the process of stretching, which eventually causes the tensile strength in the direction of gravity of electrodeposited cobalt plates to be slightly greater than the tensile strength in the horizontal direction.

From the comparison of the tensile strength of electrodeposited cobalt plates in the horizontal direction and gravity direction, the tensile strength of the A-Co plates is significantly greater than that of the other two cobalt plates. And the trend of their yield strength is the same as that of their

tensile strength, i. e. A-Co>C-Co>B-Co. This is mainly because the grain size is small with a higher number of grain boundaries, and grain boundaries in metallic materials play an important role in strengthening. Moreover, grain boundaries will restrict the movement of dislocations, thus improving the overall strength of the metallic material, from which it can be seen that the effect of grain size on strength is in accordance with the Hall-Petch relationship[27].

2.4.2 Fracture morphology

Fig. 9 shows the tensile fracture morphology of three types of electrodeposited cobalt plates in the horizontal and gravity directions. From Fig.9a and 9a', it can be seen that the fracture morphology of A-Co plates in both directions is typical of a river pattern, accompanied by a small amount of tearing ridges, which have a certain directionality. Meanwhile, the fracture is composed of a flat surface and a rough surface; the flat surface is the dissociation surface, while the rough surface is the cross-layer dissociation surface, and the gathering of these penetration dissociation surfaces will form a fracture steps[28], which indicate brittle fractures. And it can be seen that there are ball-shaped inclusions, and the particle size of the inclusions varies, which will have a certain impact on the performance of the cobalt plate[29]. The tensile fracture morphology of B-Co plates in the two directions is composed of river-pattern cleavage fractures and dimples, which belong to the brittle fracture. The plastic toughness of B-Co plates is slightly better than the plastic toughness of A-Co plates, but the strength is lower. The fracture morphology in the horizontal direction (as shown in Fig. 9c) of C-Co plates is also composed of a river pattern and a dimple, and the dimple size of C-Co plates is smaller than that of B-Co plates, indicating that its plastic toughness is worse than that of the B-Co plates, which belong to the brittle fracture. Nevertheless, the fracture morphology in the gravity direction (as shown in Fig. 9c') is a river pattern, showing a certain directionality, which is a characteristic of cleavage fracture.

2.5 Impact test at room temperature

The three types of electrodeposited cobalt plates are processed into standard Charpy V-impact small-size specimens in accordance with GB/T 229-2020. In order to make a simple comparison between the two sizes of specimens, the conversion coefficient A_{k10}:$A_{k7.5}$:A_{k5}:$A_{k2.5}$=1:0.75:0.5:0.25 of the ratio of the impact work for the large and small specimens was used for conversion [30]. It is also equivalent to the impact work consumed per unit cross section when the metal specimen is fractured by the impact load in the impact test. All three types of electrodeposited cobalt plates are sampled in different directions and different positions, and then Charpy pendulum impact tests are carried out under the same conditions and their average values are evaluated to obtain the data shown in Table 5 and Table 6.

From the data in Table 5 and Table 6, it is clear that they all have relatively low impact toughness values. The impact toughness value of A-Co plates is 22.17 J/cm^2, that of B-Co plates is 47.11 J/cm^2, and that of C-Co plates is 39.64 J/cm^2. The impact toughness of the B-Co plates is better than that of other two Co plates, while the impact toughness of the A-Co plates is the worst. As the impact test reflects the brittle fracture ability of the material, all three types of electrodeposited cobalt plates are fractured once after the Charpy pendulum impact test, indicating that the electrodeposited cobalt plates are typical brittle materials, which is consistent with the conclusion obtained from the tensile test.

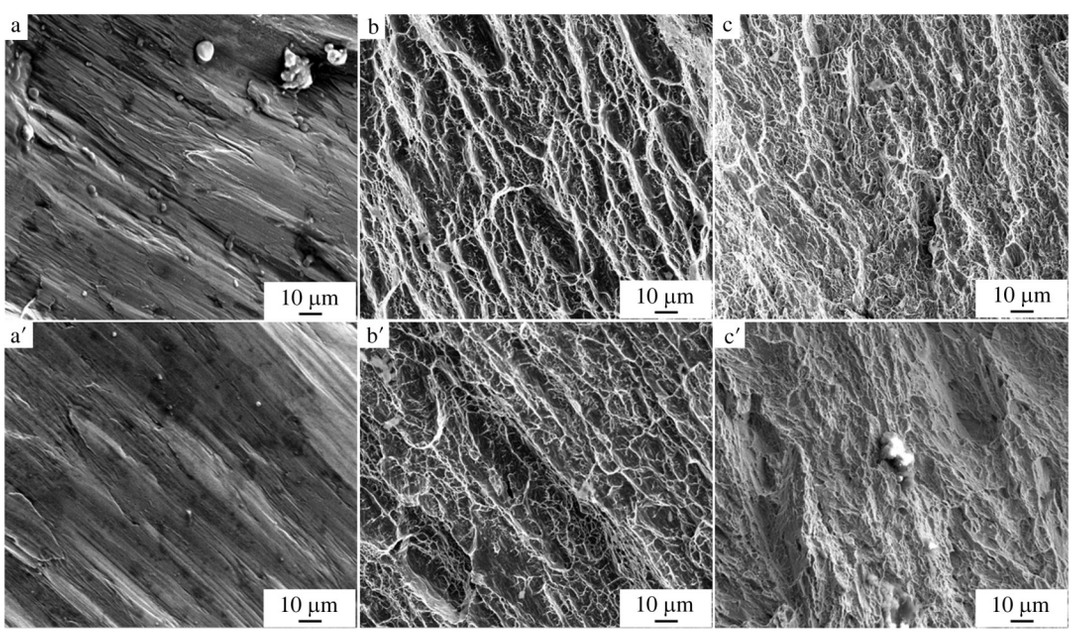

Fig.9 Tensile fracture morphologies of three electrodeposited cobalt plates in horizontal and gravity directions: (a, a') A-Co, (b, b') B-Co, and (c, c') C-Co

Table 5 Impact work and impact toughness of three electrodeposited cobalt plates

Plate			Specimen thickness/mm	Impact work, A_k/J	Impact toughness, a_k/J·cm^{-2}
A-Co	Upper	Horizontal direction	5	10.58	21.16
		Gravity direction	5	11.56	23.12
	Middle	Horizontal direction	5	9.60	19.20
		Gravity direction	5	12.64	25.28
	Lower	Horizontal direction	5	10.58	21.16
		Gravity direction	5	11.56	23.12
B-Co	Upper	Horizontal direction	5	22.25	44.50
		Gravity direction	5	25.58	51.16
	Middle	Horizontal direction	5	22.25	44.50
		Gravity direction	5	24.50	49.00
	Lower	Horizontal direction	5	22.25	44.50
		Gravity direction	5	24.50	49.00
C-Co	Upper	Horizontal direction	2.5	9.60	38.40
		Gravity direction	2.5	11.56	46.24
	Middle	Horizontal direction	2.5	9.60	38.40
		Gravity direction	2.5	9.60	38.40
	Lower	Horizontal direction	2.5	8.53	34.12
		Gravity direction	2.5	10.58	42.32

Table 6 Average values of impact work and impact toughness of three electrodeposited cobalt plates in different directions

Plate		Specimen thickness/mm	Impact work, A_k/J	Impact toughness, a_k/J·cm^{-2}	Average impact toughness, a_k/J·cm^{-2}
A-Co	Horizontal direction	5	10.25	20.50	22.17
	Gravity direction	5	11.92	23.84	
B-Co	Horizontal direction	5	22.25	44.50	47.11
	Gravity direction	5	24.86	49.72	
C-Co	Horizontal direction	2.5	9.24	36.96	39.64
	Gravity direction	2.5	10.58	42.32	

2.6 Micro-Vickers hardness

The microscopic Vickers hardness values of the three electrodeposited cobalt plates are shown in Table 7. As can be seen, there is a small difference in hardness at different positions. Furthermore, the average micro-Vickers hardness value of A-Co plates is 3681.86 MPa, that of B-Co plates is 2424.52 MPa, and that of C-Co plates is 2619.54 MPa. From the comparison of their micro-Vickers hardness values, the average micro-Vickers hardness of A-Co plates is much higher than that of B-Co and C-Co plates. And the micro-Vickers hardness value of the C-Co plates is close to that of the B-Co plates but only slightly greater than that of the B-Co plates. Su et al[6] found that the hardness of the cobalt deposited layer increases with decreasing grain size, which is consistent with the findings of this study. This trend is the same as that in the tensile strength of three electrodeposited cobalt plates, which indicates that the strength and hardness of the A-Co plates are the highest, and the strength and hardness of the B-Co plates

Table 7 Microscopic Vickers hardness values of three electrodeposited cobalt plates

Plate		Hardness, $HV_{0.2}$/×9.8 MPa	Average value, $HV_{0.2}$/×9.8 MPa
A-Co	Upper	374.6	375.7
	Middle	377.5	
	Lower	374.9	
B-Co	Upper	242.9	247.4
	Middle	256.1	
	Lower	243.1	
C-Co	Upper	267.3	267.3
	Middle	267.7	
	Lower	266.8	

are lower compared to other two types of cobalt plates.

As for B-Co and C-Co plates, the electrocrystallization behavior of cobalt can be improved by changing the processing parameters in the electro-deposition process or adding additives in the electrolyte to influence the formation rate and growth rate of crystal nuclei, resulting in a uniform and densely deposited layer with fine grains, thus improving the mechanical properties of the electrodeposited cobalt plates.

3 Conclusions

1) All three types of electrodeposited cobalt plates are pure cobalt phases with close-packed hexagonal structures. The surface and cross-section of the A-Co plates show double preferred orientation on the $(10\bar{1}0)$ and (0002) planes, while the surface of the B-Co and C-Co plates is $(10\bar{1}0)$ surfaces showing a preferred orientation, and the cross-section is (0002) surface showing a preferred orientation, indicating that the homogenization of the texture is beneficial to the grain refinement.

2) The grain size order of the three electrodeposited cobalt plates is as follows: A-Co<C-Co<B-Co, the tensile strength and micro-Vickers hardness are as follows: A-Co>C-Co>B-Co, while the impact toughness is as follows: A-Co<C-Co<B-Co. It can be seen that there is a certain connection between grain size and mechanical properties; the smaller the grain size, the higher the tensile strength and hardness, but the toughness is relatively poor. Meanwhile, the three kinds of electrodeposited cobalt plates all show the typical brittle fracture characteristics.

3) The quality of the A-Co plates is better than that of the other two electrodeposited cobalt plates.

References

1 Saha S, Sultana S, Islam M *et al*. *Ionics*[J], 2014, 20(8): 1175

2 Huang J H, Kargl Simard C, Alfantazi A M. *Canadian Metallurgical Quarterly*[J], 2004, 43(2): 163

3 Quan C, He Y. *Applied Surface Science*[J], 2015, 353: 1320

4 Bai Lan. *Synthesis and Performance Study of Deep Copper Removal Chelating Resin for Cobalt Electrolyte*[D]. Changsha: Central South University, 2012 (in Chinese)

5 Cao X, Xu L, Shi Y *et al*. *Electrochimica Acta*[J], 2019, 295: 550

6 Su F, Liu C, Zuo Q *et al*. *Materials Chemistry and Physics*[J], 2013, 139(2–3): 663

7 Ching H A, Choudhury D, Nine M J *et al*. *Science and Technology of Advanced Materials*[J], 2014, 15(1): 1

8 Patnaik P, Tripathy B C, Bhattacharya I N *et al*. *Metallurgical and Materials Transactions B*[J], 2015, 46(3): 1252

9 Luo X, Chen C Y, Chang T F M *et al*. *Journal of The Electrochemical Society*[J], 2021, 168(10): 102 502

10 Wu Xuehao. *Modification of Ion-Exchange Membrane and Its Application in Cobalt Electro-Deposition*[D]. Harbin: Harbin Institute of Technology, 2016 (in Chinese)

11 Xu Yangtao, Wang Chao, Liu Zhijian *et al*. *Rare Metal Materials and Engineering*[J], 2022, 51(4): 1462 (in Chinese)

12 Banbur-Pawlowska S, Mech K, Kowalik R *et al*. *Applied Surface Science*[J], 2016, 388: 805

13 Li M, Gao B, Shi Z *et al*. *Journal of Solid State Electrochemistry*[J], 2016, 20(1): 247

14 Patnaik P, Padhy S K, Tripathy B C *et al*. *Transactions of Nonferrous Metals Society of China*[J], 2015, 25(6): 2047

15 Mahdavi S, Allahkaram S R. *Transactions of Nonferrous Metals Society of China*[J], 2018, 28(10): 2017

16 Liu Tiancheng, Lu Zhichao, Li Deren *et al*. *Journal of Functional Materials*[J], 2007, 38(1): 138 (in Chinese)

17 Zhou Shaomin. *Metal Electro-Deposition-Principle and Research Method*[M]. Shanghai: Shanghai Science and Technology Press, 1987: 140 (in Chinese)

18 Rasmussen A A, Jensen J A D, Horsewell A *et al*. *Electro Chimica Acta*[J], 2001, 47(1–2): 67

19 Xia Tiandong, Zhang Xiaoyu, Xu Yangtao *et al*. *The Chinese Journal of Nonferrous Metals*[J], 2015, 25(11): 3133 (in Chinese)

20 Monshi A, Foroughi M R, Monshi M R. *World J Nano Sci Eng*[J], 2012, 2: 154

21 Wang Eege. *Surface Dynamics in Thin Film Growth*[M]. Beijing: Science Press, 2002: 52 (in Chinese)

22 Zhang Xiaoyu. *A Comparative Study on Several Kinds of Pure Nickel Used in Industry*[D]. Lanzhou: Lanzhou University of Technology, 2015 (in Chinese)

23 Wang Chao. *Effect of a Soluble or Insoluble Anode on the Microstructure and Properties of Electrodeposited Nickel*[D]. Lanzhou: Lanzhou University of Technology, 2021 (in Chinese)

24 Hu Gengxiang, Cai Xun, Rong Yonghua *et al*. *Fundamentals of Materials Science*[M]. Shanghai: Shanghai Jiao Tong University Press, 2010: 123 (in Chinese)

25 Liu Zhijian. *Microstructure and Grain Evolution Characteristics of the Nickel Deposited Layer by Industrial Electrolysis*[D].

Lanzhou: Lanzhou University of Technology, 2021 (in Chinese)
26 Zheng Xiulin. *Mechanical Properties of Materials*[M]. Xi'an: Northwestern Polytechnic University Press, 2000 (in Chinese)
27 Hug E, Keller C, Dubos P A *et al*. *Journal of Materials Research and Technology*[J], 2021, 11: 1362
28 Li Lei, Cao Rui, Zhang Ji *et al*. *Rare Metals*[J], 2008, 32(4): 409 (in Chinese)
29 Martin M L, Liew L A, Read D T *et al*. *Sensors and Actuators A: Physical*[J], 2020, 314: 112 239
30 Cao Shengju. *Heat Treatment*[J], 2010, 25(3): 60 (in Chinese)

电积钴板微观组织结构及力学性能对比

徐仰涛[1,2,3]，代靖民[1,2]，裴　亮[1,2]，彭　尹[1,2]，杜海洋[1,2]
(1. 兰州理工大学 省部共建有色金属先进加工与再利用国家重点实验室，甘肃 兰州 730050)
(2. 兰州理工大学 材料科学与工程学院，甘肃 兰州 730050)
(3. 兰州理工大学 白银新材料研究院，甘肃 白银 730900)

摘　要：研究了3种电积钴板的微观组织结构和力学性能之间的差异，采用X射线衍射仪和扫描电子显微镜分析了3种电积钴板的择优取向、晶体结构和微观组织形貌；并分析了3种电积钴板的强度、硬度和韧性。结果表明：3种电积钴板均是密排六方结构（hcp）的纯钴相，晶粒取向随机。A-Co板沉积层均匀致密、孔洞较少，而B-Co板和C-Co板的沉积层较为分散且存在大量的孔洞。同时A-Co板表面的平均晶粒尺寸最小，沉积层晶粒大小分布均匀，B-Co板表面的平均晶粒尺寸最大，沉积层晶粒大小分布不均匀。3种电积钴板截面的始极片都是柱状晶结构，且始极片两侧的生长方式不同。由力学性能分析发现A-Co板的抗拉强度和硬度均高于其它2种钴板，但是韧性较差。综上所述，A-Co板的品质要明显优于B-Co板和C-Co板的品质。

关键词：电积钴；晶粒尺寸；晶体结构；力学性能；择优取向

作者简介：徐仰涛，男，1978年生，博士，教授，兰州理工大学材料科学与工程学院，甘肃 兰州 730050，电话：0931-2973939，E-mail：xuyt@lut.edu.cn